

peptides such as CAMP<sup>18</sup>. Thus, our results suggest that upregulated VDR expression during *Mtb* infection in HCs triggers the increased expression of CAMP and other antimicrobial peptides. Increased expression of cathelicidin has also been reported to activate the transcription of autophagy-related genes, *Beclin-1* and *Atg5*. Autophagy is reported to be an important host defence mechanism against *Mtb*<sup>8</sup>. Thus, vitamin D<sub>3</sub> might serve to restrict the growth of *Mtb* through multiple mechanisms.

In conclusion, the results suggest that vitamin D<sub>3</sub> up-regulates the antimicrobial peptides CAMP and DEF- $\alpha$ 3 during *Mtb* infection, which may be detrimental to *Mtb* and may probably be eliminated by neutrophils through the mechanism of autophagy. Moreover, administration of vitamin D<sub>3</sub> as a nutritional supplementation during anti-TB treatment may be an useful adjunct therapy for the disease.

14. Tan, B. H. *et al.*, Macrophages acquire neutrophil granules for antimicrobial activity against intracellular pathogens. *J. Immunol.*, 2006, **177**, 1864–1871.
15. Blomgran, R., Desvignes, L., Briken, V. and Ernst, J. D., *Mycobacterium tuberculosis* inhibits neutrophil apoptosis, leading to delayed activation of naive CD4 T cells. *Cell Host Microbe*, 2012, **11**, 81–90.
16. Zhu, L. M. *et al.*, Multidrug-resistant tuberculosis is associated with low plasma concentrations of human neutrophil peptides 1–3. *Int. J. Tuberc. Lung Dis.*, 2011, **15**, 369–374.
17. Sonawane, A. *et al.*, Cathelicidin is involved in the intracellular killing of mycobacteria in macrophages. *Cell. Microbiol.*, 2011, **13**, 1601–1607.
18. Liu, P. T. *et al.*, Toll-like receptor triggering of a vitamin D-mediated human antimicrobial response. *Science*, 2006, **311**, 1770–1773.

ACKNOWLEDGEMENTS. K.A. thanks the Indian Council for Medical Research, New Delhi for providing senior research fellowship.

Received 22 October 2013; revised accepted 19 May 2014

1. Kobayashi, K., Allred, C., Castriotta, R. and Yoshida, T., Strain variation of bacillus Calmette-Guerin-induced pulmonary granuloma formation is correlated with anergy and the local production of migration inhibition factor and interleukin 1. *Am. J. Pathol.*, 1985, **119**, 223–235.
2. Ganz, T. *et al.*, Defensins. Natural peptide antibiotics of human neutrophils. *J. Clin. Invest.*, 1985, **76**, 1427–1435.
3. Fu, L. M., The potential of human neutrophil peptides in tuberculosis therapy. *Int. J. Tuberc. Lung Dis.*, 2003, **7**, 1027–1032.
4. Cowland, J. B., Johnsen, A. H. and Borregaard, N., hCAP-18, a cathelin/pro bactenecin like protein of human neutrophil specific granules. *FEBS Lett.*, 1995, **368**, 173–176.
5. Zanetti, M., Gennaro, R. and Romeo, D., The cathelicidin family of antimicrobial peptide precursors: a component of the oxygen-independent defense mechanisms of neutrophils. *Ann. NY Acad. Sci.*, 1997, **832**, 147–162.
6. Nursyam, E. W., Amin, Z. and Rumende, C. M., The effect of vitamin D as supplementary treatment in patients with moderately advanced pulmonary tuberculous lesion. *Acta Med. Indones.*, 2006, **38**, 3–5.
7. Liu, P. T., Stenger, S., Tang, D. H. and Modlin, R. L., Cutting edge: vitamin D-mediated human antimicrobial activity against *Mycobacterium tuberculosis* is dependent on the induction of cathelicidin. *J. Immunol.*, 2007, **179**, 2060–2063.
8. Yuk, J. M. *et al.*, Vitamin D<sub>3</sub> induces autophagy in human monocytes/macrophages via cathelicidin. *Cell Host Microbe*, 2009, **6**, 231–243.
9. Selvaraj, P., Prabhu Anand, S., Harishankar, M. and Alagarasu, K., Plasma 1,25 dihydroxy vitamin D<sub>3</sub> level and expression of vitamin D receptor and cathelicidin in pulmonary tuberculosis. *J. Clin. Immunol.*, 2009, **29**, 470–478.
10. Provedini, D. M., Tsoukas, C. D., Deftos, L. J. and Manolagas, S. C., 1,25-dihydroxyvitamin D<sub>3</sub> receptors in human leukocytes. *Science*, 1983, **221**, 1181–1183.
11. Takahashi, K. *et al.*, Human neutrophils express messenger RNA of vitamin D receptor and respond to 1 $\alpha$ ,25-dihydroxyvitamin D<sub>3</sub>. *Immunopharmacol. Immunotoxicol.*, 2002, **24**, 335–347.
12. Wang, T. T. *et al.*, 1,25-Dihydroxy vitamin D<sub>3</sub> is a direct inducer of antimicrobial peptide gene expression. *J. Immunol.*, 2004, **173**, 2909–2912.
13. Chandra, G. *et al.*, Effect of vitamin D<sub>3</sub> on phagocytic potential of macrophages with live *Mycobacterium tuberculosis* and lymphoproliferative response in pulmonary tuberculosis. *J. Clin. Immunol.*, 2004, **24**, 249–257.

## *In situ* formation of silver nanowire networks on paper

Shravan Kumar Parmar and Venugopal Santhanam\*

Department of Chemical Engineering, Indian Institute of Science, Bangalore 560 012, India

**Simple, universally adaptable techniques for fabricating conductive patterns are required to translate laboratory-scale innovations into low-cost solutions for the developing world. Silver nanostructures have emerged as attractive candidates for forming such conductive patterns. We report here the *in situ* formation of conductive silver-nanowire networks on paper, thereby eliminating the need for either cost-intensive ink formulation or substrate preparation or complex post-deposition sintering steps. Reminiscent of the photographic process of ‘salt printing’, a desktop office printer was used to deposit desired patterns of silver bromide on paper, which were subsequently exposed to light and then immersed in a photographic developer. Percolating silver nanowire networks that conformally coated the paper fibres were formed after 10 min of exposure to light from a commercial halogen lamp. Thus, conductive and patterned films with sheet resistances of the order of 4  $\Omega/\square$  can be easily formed by combining two widely used processes – inkjet printing and photographic development.**

**Keywords:** Conductive patterns, inkjet printing, paper electronics, photographic development, silver nanowire.

\*For correspondence. (e-mail: venu@chemeng.iisc.ernet.in)

PAPER is an inexpensive and easily available material that is rapidly emerging as a substrate of choice for the fabrication of disposable electronic circuits<sup>1</sup> and point-of-care diagnostic devices<sup>2</sup>. Batteries<sup>3</sup>, field-effect transistors<sup>4</sup>, RFID antennas<sup>5</sup>, sensors<sup>6</sup> and solar cells<sup>7</sup> have been fabricated on paper-based substrate, wherein paper functions primarily as a mechanical support and sometimes as an active part of the device<sup>8</sup>. Significant efforts are underway, in the field of paper electronics, to develop additive manufacturing techniques in order to reduce material consumption and lower costs<sup>9</sup>. Digital inkjet printing is a widely available technological platform that allows complete flexibility during pattern designing while also being compatible with the use of paper<sup>10</sup>, attributes that can promote rapid penetration of laboratory-scale innovations in the developing world.

Conductive layers, either as interconnects or active elements, are an integral part of all electrical and electronic circuits. As such, there is significant research on printing conductors using different materials<sup>11–13</sup>. Amongst them, silver has emerged as the material of choice since it is the best conductor that is also stable under normal operating conditions<sup>14,15</sup>. Functional inks for printing silver can be classified into three main categories, namely organometallic inks<sup>16,17</sup>, complexed silver salt-based ink formulations<sup>18–20</sup>, and nanoparticle-based inks<sup>21–23</sup>. Organometallic inks form silver on the substrate by decomposition of the deposited ink upon heating. The considerable energy input required to decompose organometallic inks limits their usefulness for paper-based applications. Ink formulations containing silver salts in complexed form along with appropriate reducing agents can form overlapping silver nanostructures *in situ* upon drying. Such inks can be used for either printing or ‘writing’. The high conductivities, equivalent to that of bulk silver, achieved using such inks are promising for various applications; however, the tedious processing and short shelf-life of these inks limit their suitability for low-cost applications<sup>19,24</sup>. Silver nanoparticle inks are the most widely prevalent form of conductive inks that are also commercially available. Curing of these inks to form conductive traces by chemical or physical processing is a crucial step in obtaining conductive traces. Significant efforts have been undertaken to develop rapid curing techniques<sup>15,16,21,22,24–27</sup>. Recently, desktop printing compatible ink-substrate packs have become available<sup>6,28</sup>. Despite such efforts, the technologically intensive processing required to formulate these inks and the smooth substrates required remain prohibitively expensive for widespread adaptation.

During a preliminary search for a simple, low-cost process to form conductive patterns on paper using reactive inkjet printing, we realized that a key step for success would be the ability to avoid leaving by-products of the metallization reaction as a solid residue within the film. Photographic processing is one such metallization

scheme that relies on forming silver halide layers on a substrate, exposing silver halides to light to form a latent image, followed by ‘development’ in an appropriate chemical bath to amplify the latent image<sup>29</sup>. ‘Salt printing’ is a silver-based photographic process that relies on *in situ* formation of silver halide layers on paper and is the precursor of the modern photographic-film based process<sup>30</sup>. Therefore, we hypothesized that overexposing densely-packed silver halide layers formed *in situ* on paper using a desktop printer, followed by development could be a simple solution for forming patterned and conductive silver layers on paper, while also avoiding unwanted residues. To test this hypothesis, we used an office inkjet printer for defining patterns of silver halide layers on paper by sequentially printing aqueous solutions of potassium halide and silver nitrate. After sufficient light exposure and development, we discovered that dense percolating networks of silver nanowires were formed on paper and that conductive layers with sheet resistances of the order of a few  $\Omega/\square$  could be easily obtained using this method. In the present communication, we report the results of structural characterization of the silver nanowire networks formed on paper using such a ‘print–expose–develop’ process, posit a plausible mechanism for the formation of inter-connected silver nanowires, and demonstrate the percolating nature of the conductive films formed on paper. Recently, formation of conductive films on smooth polymer or paper substrates starting with silver nanowire containing pastes/inks have been reported<sup>31,32</sup>. Silver grains generated within the photographic film after light exposure and development have also been used as seeds to form metallic structures<sup>33</sup>. However, *in situ* formation of conductive silver nanowire networks on paper has not been reported so far.

DI water was used to prepare all the solutions. All chemicals used were of analytical grade or higher purity. The molar ratio of KX to  $\text{AgNO}_3$  printed was 2 : 1, to ensure complete conversion to  $\text{AgX}$  on the paper. For the results reported here, a bromide : iodide :: 95 : 5 wt% composition was used as the halide (X) source, as addition of iodide ions enhances photosensitivity<sup>29</sup>. Typically, 3.3 M KX and 1.67 M  $\text{AgNO}_3$  solutions (corresponding to a silver nitrate loading of 1.04  $\text{mg}/\text{cm}^2$  after three prints) were used to prepare the samples reported here, except in the case where  $\text{AgNO}_3$  concentration was varied from 0.167 to 1.67 M, while KX values varied from 0.33 to 3.3 M, correspondingly. The developer solution was prepared according to a standard recipe for making D-76 (ref. 34). Briefly, 100 g of sodium sulphite was dissolved in hot water (50°C) and then 2 g of metol (monomethyl-*p*-aminophenol hemisulphate) along with 5 g of hydroquinone were added and mixed thoroughly. To this solution, 2 g of borax was added. Finally, cold water was added to make the solution volume 1000 ml. The pH of the D-76 developer was found to be 8.5. (The use of ascorbic acid also led to the formation of nanowire films, but with

conductivity values that were 50% in comparison to those films formed using D-76.) The washing or 'fixing' solution consisted of 0.5 M hypo solution (sodium thiosulphate).

A HP Deskjet 1000 printer was used for printing the precursor salt solutions. Two separate HP 802 black ink cartridges were used for printing KX and AgNO<sub>3</sub> solutions. The cartridges were thoroughly cleaned by making a hole in their lids, removing the sponge holding the black ink and rinsing the reservoir in flowing tap water. Finally, DI water was filled in the reservoir and some test patterns were printed on paper until there was no evidence of black ink on paper. Black and white designs were generated using a vector graphics editor (Inkscape, an open source graphics editor) and printed at 600 dpi resolution. By weighing the cartridges before and after printing DI water, the volume of solution deposited was found to be 1.2  $\mu\text{l}/\text{cm}^2$  of the printed area. To ensure spatial uniformity of the printed material, all patterns were generated using three consecutive prints of the salt solutions. After printing the desired amounts of potassium halide and silver nitrate solutions, the paper (A4 copier paper, 80 gsm) was kept at a distance of 50 cm under a 500 W halogen lamp (Crompton Greaves J240V 500 W R7S, 9500 Lumens) for 10 min (exposure to either sunlight on a summer afternoon in Bangalore for 1.5 h or an UV lamp (8 W, 254 nm) for 10 min also produced films with similar conductivities). Longer exposure times did not affect the measured conductivity appreciably, while shorter exposures (5 min) led to films with nonuniform conductivities and large fluctuations in measured resistance values over length scales of a few millimetres. The samples were placed in a plastic tray containing a standard developer solution (D-76, containing metol) for 10 min, followed by washing in a tray containing a fixer for 10 min to remove unreacted silver ions, if any (fixing does not alter the conductivity of the features). The paper was then rinsed in water and allowed to dry under ambient conditions or dried using a hair drier.

For the solution synthesis of silver nanowires, 1 ml silver nitrate solution (0.25 M) was mixed with 2 ml KBr/KI solution (0.25 M). After the desired extent of light exposure, 3 ml of D-76 developer was added and the solution was left to stand for 10 min. If the solution had been previously exposed to light, it turned greenish-brown in colour indicating the formation of silver nanostructures. The excess developer was then removed by decantation following a centrifugation step. The precipitate was then soaked in hypo solution for 10 min to remove unreacted silver ions and then rinsed with DI water. Finally, the precipitate was dispersed in DI water using a sonicator followed by drop casting on a silicon wafer for FESEM analysis.

Field emission scanning electron microscope (FESEM) images were obtained using secondary electrons (Everhart-Thornley SE detector (Zeiss Ultra-55)). The operating

voltage was typically 5 kV, and working distance was 6–7 mm. Movies were collected as a series of scanned frames using an add-on in the FESEM software. XRD characterization of the samples was carried out using a diffractometer (Philips X'pert Pro). The scan range was 20°–80° ( $2\theta$  values). Photographs of samples and movies on capacitive switching were captured using a digital camera. A four-point probe station (Model 280DI, Four Dimensions Inc.) was used to determine the sheet resistance of the samples. The samples for sheet resistance measurement consisted of two 6 cm squares printed on an A4 paper. The average value of the readings taken at different positions on the two squares was reported. For the bending tests, one bending cycle consisted of manually flexing the paper up and down (i.e. into 3 and 4 shape). The resistance data were measured after every 50 such cycles till a total of 1000 cycles. The test sample consisted of two squares (side length of 14 mm each) that acted as contacts to three conductive lines (1 mm width  $\times$  12 mm length). The minimum radius of curvature during the bending cycles was nominally 3 mm.

A desktop inkjet printer was used to sequentially deposit potassium halide and silver nitrate solutions on paper in the desired patterns (Figure 1 *a*). Polygonal crystals were found to be dispersed evenly on all the fibres in the printed portions of the paper (Figure 1 *b*, top panel). XRD analysis of the film formed on paper, prior to light exposure, indicates the presence of FCC crystals, whose major reflections could be assigned to AgBr as shown (ICCD: 04-006-5963, Figure 1 *c*, top panel). The other reflections could be assigned to CaCO<sub>3</sub> (ICCD: 04-007-2808), which is attributed to the use of calcite as a filler in office paper. The printed film on paper has a greenish tint (Figure 1 *d*, left) and there was no evidence of electrical connectivity on a macroscopic scale in these features. The printed film on paper was then exposed to light from a halogen lamp for 10 min, which should lead to the formation of silver clusters within the halide crystals. The paper was then sequentially immersed in a developing bath and a fixing bath. Interconnected network of silver nanowires, whose diameters ranged from 30 to 100 nm, were found on all the printed portions of the paper (Figure 1 *b*, lower panel). The tangled network morphology was observed in both planar and cross-sectional views, and the thickness of the nanowire film was similar to that of the polygonal crystals found prior to development, suggesting that AgBr crystals had disintegrated into this tangled network after light exposure and development. XRD analysis of these films of nanowires showed reflections that were assigned to FCC silver (ICCD: 04-006-2775, Figure 1 *c*, lower panel), alongside the reflections attributable to calcite. Remarkably, the film showed excellent conductivity over macroscopic length scales. The film had a dull brown appearance, due to its rough texture and penetration into the paper. The as-fabricated silver films showed excellent adhesion to the paper fibres and

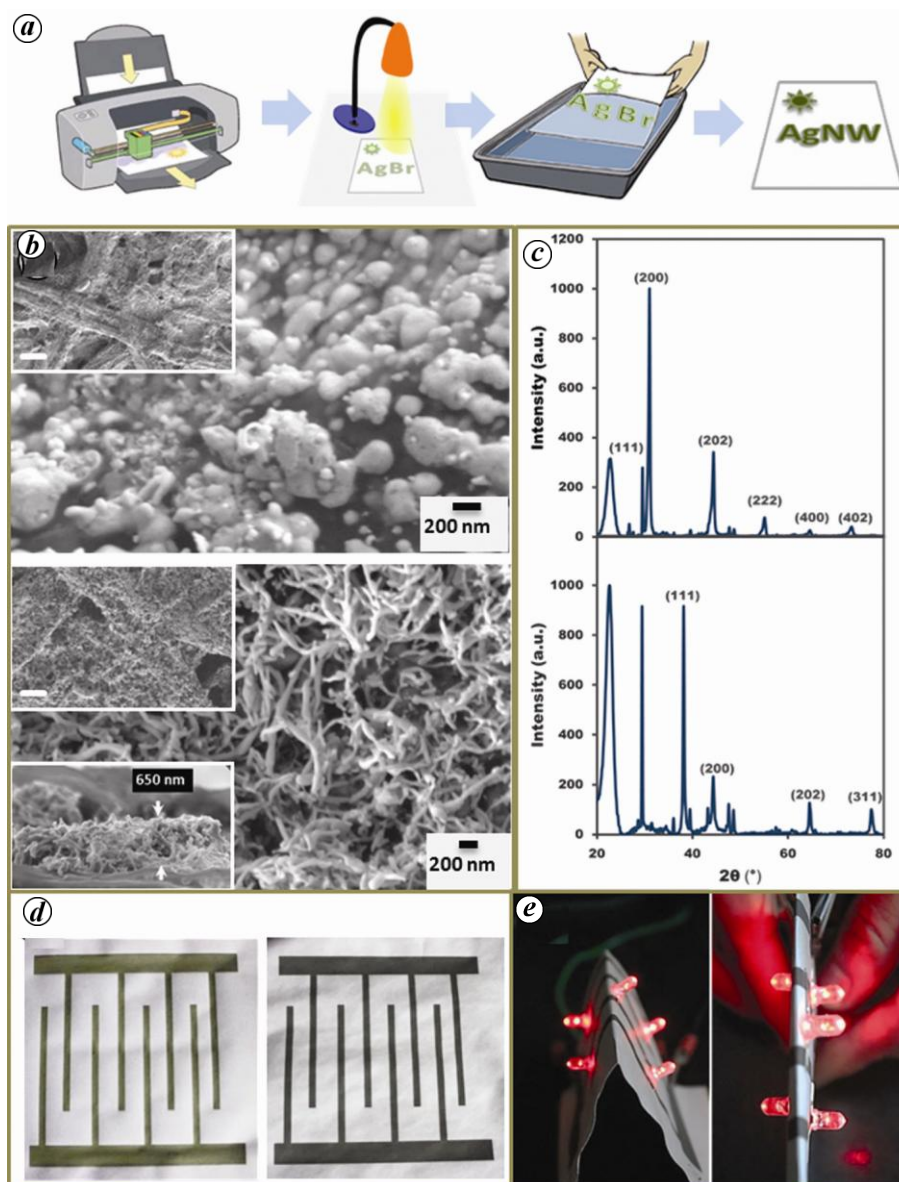


**Figure 1.** *a*, Schematic representation of the print–expose–develop cycle. *b*, FESEM images of the film after printing (top panel) and after light exposure and development (bottom panel). (Insets, Top-left corner, top and bottom panels) Lower magnification images showing coated paper-fibres. Scale bars correspond to 10  $\mu\text{m}$ . (Inset, Bottom-left corner of the bottom panel) Cross-sectional view of the conductive film. *c*, XRD of the films formed on paper after printing (top panel) and after developing and fixing (bottom panel). *d*, Digital photographs of a printed electrode pattern after salt printing (left) and after developing and fixing (right). The distance between the thicker horizontal electrodes is 15 cm. *e*, The paper substrate could be bent or folded flat without losing connectivity. The LED pins were ‘stapled’ to make electrical contact.

could not be scraped or peeled off without damaging the underlying paper fibres. The excellent connectivity across the conductive film is further demonstrated by creasing to form a flatly folded electrode (Figure 1 *e*). A touch-sensitive capacitive switch was also fabricated for demonstration purposes ([Supplementary Information movie 1; see online](#)).

Silver nanowires were found to emanate from the surface of AgBr crystals during FESEM imaging of silver halide films that were earlier exposed to light from the

halogen lamp (Figure 2 *a* and *b*, and [Supplementary Information movie 2; see online](#)). The AgBr films remained unchanged under similar imaging conditions if they were not exposed to light prior to imaging. AgBr crystals are known to have highly mobile  $\text{Ag}^+$  species within their lattice. During photographic development, the silver clusters formed upon light exposure act as an electron reservoir that helps reduce mobile silver ions in the lattice, thereby, amplifying the ‘latent image’<sup>35</sup>. We hypothesize that a similar process occurs during the

print–expose–develop process presented here, as well as during FESEM imaging. Clearly, the electrons used for imaging have reduced the silver ions within the polygonal AgBr crystals to form nanowires; a process catalysed by the creation of ‘latent silver clusters’ during light exposure. Similar filamentous outgrowth of wire-like silver offshoots has been reported in an earlier electron microscopic observation of AgBr films<sup>36</sup>.

To understand the effect of the substrate and the extent of light exposure on nanowire formation, we carried out three experiments in solution, as described earlier, by adding developing and fixing agent sequentially to freshly made silver bromide solutions that had been kept: (i) in a covered vial during the experiment which was carried out in a dark room; (ii) in a vial exposed to ambient fluorescent lighting during the experiment, and (iii) in a vial that was exposed to light from the halogen lamp for 10 min, prior to the addition of developing solution. Silver nanowires formed in solution only upon being exposed to light from the halogen lamp. In the sample exposed to ambient light, polyhedral particles were predominantly formed; whereas in the sample kept in the dark, washing in ‘hypo’ solution led to complete dissolution of the precipitate, indicating that reduction of silver had not taken place at all. These results confirm that higher dosage of light exposure is the key for nanowire formation, while also dispelling doubts regarding the role of unknown chemical species present in the office paper. An earlier study<sup>37</sup> on the formation of silver nanowires from silver bromide crystals after exposure to ambient light found that nanowires were only formed if gelatin was used to stabilize the AgBr emulsion and when excess silver nitrate was also present in the solution. The role of gelatin has been speculated to be similar to that of PVP<sup>38</sup>, which acts as a template that controls crystal growth by passivating certain crystal facets. However, such a mechanism cannot account for either the fact that nanowires were formed in the absence of gelatin or the role of light exposure in nanowire formation. Given that several ‘latent sites’ can be formed upon intense light exposure<sup>29</sup>, we postulate that reduction of mobile silver ions at multiple sites on a grain leads to break-up of the parent AgBr crystal into silver nanowires, some of which can also grow and span across crystals. Silver nanowires bridging across to touch neighbouring AgBr crystals can induce metallization of the neighbouring crystals, and thus explain the creation of macroscopically interconnected networks from silver bromide layers that were non-overlapping at the microscopic scale. This mechanism is also consistent with earlier reports on the formation of silver filaments from individual silver bromide crystals<sup>36,39</sup> under conditions similar to those used in our study (i.e. chemical development, wherein only silver ions from the parent silver bromide crystal are reduced). Interestingly, a recent report demonstrates the formation of silver chloride crystals decorated with silver nanoparticle

nuclei during the ‘waiting period under ambient light conditions’ that is part of the standard high-temperature polyol route<sup>40</sup>. Our results on the dosage of light exposure suggest that controlling light exposure may be a fruitful avenue towards room-temperature silver nanowire synthesis in the polyol process.

A percolation threshold for macroscopic electrical connectivity was observed in the variation of sheet resistance as a function of silver nitrate loading (Figure 3). Beyond a threshold value of the amount of silver nitrate printed, the sheet resistance dropped sharply by five orders of magnitude from  $10^8$  to  $10^3 \Omega/\square$ . The post-threshold behaviour of the sheet resistance data could be fitted reasonably well using a model based on percolation theory (eq. 1), which describes the creation of long-range conductive channels in randomly dispersed systems.

$$\rho_s = \frac{1}{A \left( \frac{\omega}{\omega_c} - 1 \right)^\alpha}, \quad (1)$$

wherein  $\rho_s$  represents the sheet resistance ( $\Omega/\square$ ) beyond the percolation threshold,  $A$  is a proportionality constant,  $\omega$  represents the amount of silver nitrate printed,  $\omega_c$  denotes a critical threshold value for the amount of silver nitrate ( $130 \pm 20 \mu\text{g}/\text{cm}^2$ , as estimated using a nonlinear curve fit)<sup>41</sup>, and  $\alpha$  is a scaling exponent that depends on the dimensionality of the system (estimated to be  $2.2 \pm 0.3$ ). The estimated range of the scaling exponent (95% confidence levels) encompasses the value of 1.94 expected of a 3D percolating network<sup>42</sup>. This result is in accord with the entangled nanowire features observed throughout the depth of the conductive film. The inset in Figure 3 demonstrates the power-law scaling of the sheet resistance values close to the threshold. An implicit assumption in deriving eq. (1) is that an increase in the amount of silver nitrate printed does not change the film thickness; a breakdown of this assumption at higher values of silver nitrate loading could be the cause of the deviations observed. The specific conductivity of the as-fabricated submicron thick silver films is in the range 1–10% of the bulk silver value of  $6.3 \times 10^7 \text{ S}/\text{m}$ , a range that depends on the estimates of porosity of the system as well as the amount of silver present on the top surface of paper. We believe that macroscopic conductivity can be enhanced by further optimizing the salt concentrations to form 2–3  $\mu\text{m}$  sized tabular crystals of AgBr on paper, such that the resultant nanowires can more efficiently span the regions where large cellulose fibres (5–10  $\mu\text{m}$  dia.) cross over each other. In comparison, films fabricated using inkjet printing of a specially formulated silver nanoparticle ink followed by plasma and microwave sintering are reported to have 60% of the bulk specific conductivity, albeit on smooth plastic substrates<sup>27</sup>. Figure 4 shows the variation of resistance (scaled to the initial value) as a

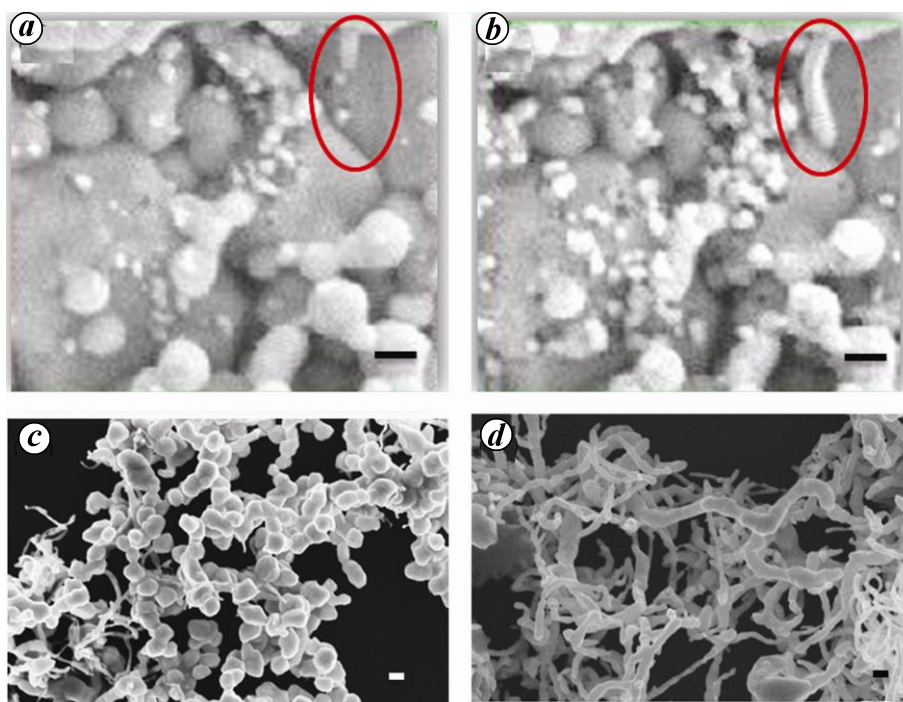


**Figure 2.** Effect of light exposure on nanowire growth. *a, b*, FESEM images from subsequent scans ( $\Delta t = 5$  s) during imaging of an AgBr sample on paper that was exposed to light from a halogen lamp. The oval outline highlights the growth of a nanowire during imaging. *c*, Silver nanostructures formed in solution after exposure to ambient light. *d*, Silver nanostructures formed in solution after 10 min of exposure to light from a halogen lamp. All scale bars correspond to 200 nm.

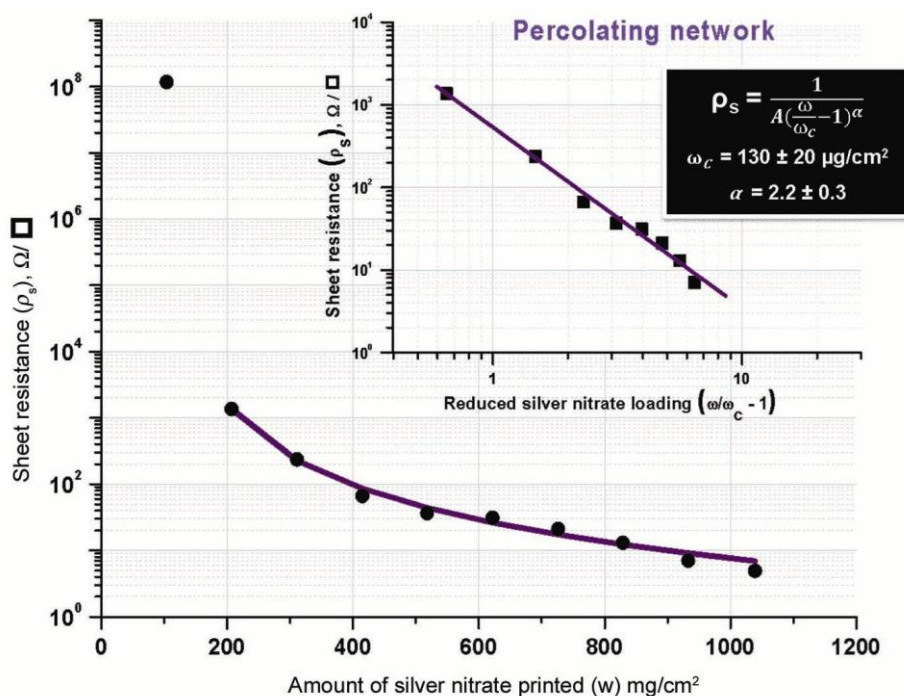


**Figure 3.** Variation of the measured sheet resistance ( $\rho_s$ ) as a function of the amount of silver nitrate printed ( $\omega$ ). The sharp decline in sheet resistance between the first two data points indicates the presence of a critical threshold value for silver nitrate loading ( $\omega_c$ ) to form a percolating conductive network. (Inset) A log–log plot of the sheet resistance as a function of reduced silver nitrate loading (i.e. loading normalized with respect to the critical value). Only data points beyond the threshold are considered in the inset plot. The points represent the measured data while the curves represent a model fit (based on a nonlinear curve fit) to the equation based on percolation theory. The model used as well as the estimated parameter values (mean  $\pm$  standard error) for critical loading and scaling exponent are shown.

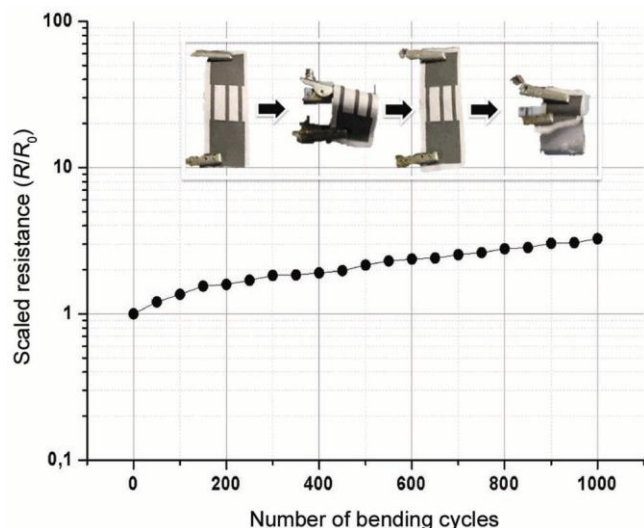


**Figure 4.** Variation of the scaled resistance ( $R/R_0$ ) as a function of the number of bending cycles. The points represent the data collected after every 50 cycles. The line is a guide to the eye. (Inset) Digital photographs of the sample under test being bent during one complete cycle.

function of the number of bending cycles. It is seen that the resistance varies only by a factor of three over 1000 cycles, which attests to the excellent adhesion and conformal coverage of the silver nanowires.

In conclusion, a simple process, comprising of print–expose–develop sequence, for the *in situ* formation of silver nanowire networks on paper has been demonstrated. The process does not require any surface modification of the paper and the inherent characteristic of standard office paper to absorb aqueous ink has been leveraged to form highly conductive patterned features within minutes. The fact that two simple and widely used processes, inkjet printing and photographic development can be combined to form conductive patterns on paper without requiring substantial capital or running costs should encourage the widespread adaptation of low-cost, disposable diagnostic and electrical devices, especially in the developing world. Furthermore, the discovery of the importance of light exposure in forming nanowires from AgBr crystals will be useful in optimizing the process of silver nanowire formation in solution.

- Irimia-Vladu, M., Głowacki, E. D., Voss, G., Bauer, S. and Sariciftci, N. S., Green and biodegradable electronics. *Mater. Today*, 2012, **15**, 340–346.
- Steckl, A. J., Circuits on cellulose. *IEEE Spectrum*, 2013, **50**, 48–61.
- Hu, L., Choi, J. W., Yang, Y., Jeong, S., La Mantia, F., Cui, L.-F. and Cui, Y., Highly conductive paper for energy-storage devices. *Proc. Natl. Acad. Sci. USA*, 2009, **106**, 21490–21494.
- Thiemann, S., Sachnov, S. J., Pettersson, F., Bollström, R., Österbacka, R., Wasserscheid, P. and Zaumseil, J., Cellulose-based ionogels for paper electronics. *Adv. Funct. Mater.*, 2013; doi: 10.1002/adfm.201302026.
- Rida, A., Yang, L., Vyas, R. and Tentzeris, M. M., Conductive inkjet-printed antennas on flexible lowcost paper-based substrates

for rfid and wsn applications. *IEEE Antenn. Propag. Mag.*, 2009, **51**, 13–23.

- Gong, N.-W., Hodges, S. and Paradiso, J. A., Leveraging conductive inkjet technology to build a scalable and versatile surface for ubiquitous sensing. In Proceedings of the 13th International Conference on Ubiquitous Computing, ACM, Beijing, China, 2011, pp. 45–54.
- Hübner, A. *et al.*, Printed paper photovoltaic cells. *Adv. Energy Mater.*, 2011, **1**, 1018–1022.
- Fortunato, E., Correia, N., Barquinha, P., Pereira, L., Gonçalves, G. and Martins, R., High-performance flexible hybrid field-effect transistors based on cellulose fiber paper. *IEEE Electron. Device Lett.*, 2008, **29**, 988–990.
- Tobjork, D. and Osterbacka, R., Paper electronics. *Adv. Mater.*, 2011, **23**, 1935–1961.
- Teichler, A., Perelaer, J. and Schubert, U. S., Inkjet printing of organic electronics – comparison of deposition techniques and state-of-the-art developments. *J. Mater. Chem. C*, 2013, **1**, 1910–1925.
- Vaseem, M., Lee, K. M., Hong, A.-R. and Hahn, Y.-B., Inkjet printed fractal-connected electrodes with silver nanoparticle ink. *ACS Appl. Mater. Interfaces*, 2012, **4**, 3300–3307.
- Tortorich, R. P. and Choi, J.-W., Inkjet printing of carbon nanotubes. *Nanomaterials*, 2013, **3**, 453–468.
- Secor, E. B., Prabhumirashi, P. L., Puntambekar, K., Geier, M. L. and Hersam, M. C., Inkjet printing of high conductivity, flexible graphene patterns. *J. Phys. Chem. Lett.*, 2013, **4**, 1347–1351.
- Perelaer, J. *et al.*, Printed electronics: the challenges involved in printing devices, interconnects, and contacts based on inorganic materials. *J. Mater. Chem.*, 2010, **20**, 8446–8453.
- Xu, L., Yang, G., Jing, H., Wei, J. and Han, Y., Pressure-assisted low-temperature sintering for paper-based writing electronics. *Nanotechnology*, 2013, **24**, 355204.
- Perelaer, J., Hendriks, C. E., Laat, A. W. M. D. and Schubert, U. S., One-step inkjet printing of conductive silver tracks on polymer substrates. *Nanotechnology*, 2009, **20**, 165303.
- Fritsch, J., Schumm, B., Biedermann, R., Grothe, J. and Kaskel, S., A new silver-based precursor as ink for soft printing techniques. *Eur. J. Inorg. Chem.*, 2012, **2012**, 878–883.
- Wu, Y. L., Li, Y. N. and Ong, B. S., A simple and efficient approach to a printable silver conductor for printed electronics. *J. Am. Chem. Soc.*, 2007, **129**, 1862–1863.
- Walker, S. B. and Lewis, J. A., Reactive silver inks for patterning high-conductivity features at mild temperatures. *J. Am. Chem. Soc.*, 2012, **134**, 1419–1421.
- Tao, Y., Tao, Y. X., Wang, B. B., Wang, L. Y. and Tai, Y. L., A facile approach to a silver conductive ink with high performance for macroelectronics. *Nanoscale Res. Lett.*, 2013, **8**, 1–6.
- Perelaer, J., de Gans, B. J. and Schubert, U. S., Ink-jet printing and microwave sintering of conductive silver tracks. *Adv. Mater.*, 2006, **18**, 2101–2104.
- Grouchko, M., Kamyshny, A., Mihailescu, C. F., Anghel, D. F. and Magdassi, S., Conductive inks with a ‘built-in’ mechanism that enables sintering at room temperature. *ACS Nano*, 2011, **5**, 3354–3359.
- Lee, Y. I., Kim, S., Jung, S. B., Myung, N. V. and Choa, Y. H., Enhanced electrical and mechanical properties of silver nanoplatelet-based conductive features direct printed on a flexible substrate. *ACS Appl. Mater. Interfaces*, 2013, **5**, 5908–5913.
- Chen, S.-P., Kao, Z.-K., Lin, J.-L. and Liao, Y.-C., Silver conductive features on flexible substrates from a thermally accelerated chain reaction at low sintering temperatures. *ACS Appl. Mater. Interfaces*, 2012, **4**, 7064–7068.
- Perelaer, J. and Schubert, U. S., Alternative sintering approaches for fast sintering of inkjet printed nanoparticles for r2r applications. In MRS Proceedings, Cambridge University Press, vol. 1400; DOI:10.1557/opl.2012.90.

26. Magdassi, S., Grouchko, M., Berezin, O. and Kamyshny, A., Triggering the sintering of silver nanoparticles at room temperature. *ACS Nano*, 2010, **4**, 1943–1948.
27. Perelaer, J., Jani, R., Grouchko, M., Kamyshny, A., Magdassi, S. and Schubert, U. S., Plasma and microwave flash sintering of a tailored silver nanoparticle ink, yielding 60% bulk conductivity on cost-effective polymer foils. *Adv. Mater.*, 2012, **24**, 3993–3998.
28. Kawahara, Y., Hodges, S., Cook, B. S., Zhang, C. and Abowd, G. D., Instant inkjet circuits: lab-based inkjet printing to support rapid prototyping of ubicomputing devices. In Proceedings of the 2013 ACM International Joint Conference on Pervasive and Ubiquitous Computing, Zurich, Switzerland, 2013, pp. 363–372.
29. Hamilton, J. F., The silver halide photographic process. *Adv. Phys.*, 1988, **37**, 359–441.
30. Talbot, H. F., Improvement in photographic pictures. US Patent 5171, 1847.
31. Wu, J.-T., Lien-Chung Hsu, S., Tsai, M.-H., Liu, Y.-F. and Hwang, W.-S., Direct ink-jet printing of silver nitrate–silver nanowire hybrid inks to fabricate silver conductive lines. *J. Mater. Chem.*, 2012, **22**, 15599–15605.
32. Nogi, M., Komoda, N., Otsuka, K. and Sugauma, K., Foldable nanopaper antennas for origami electronics. *Nanoscale*, 2013, **5**, 4395–4399.
33. Deng, T., Arias, F., Ismagilov, R. F., Kenis, P. J. and Whitesides, G. M., Fabrication of metallic microstructures using exposed, developed silver halide-based photographic film. *Anal. Chem.*, 2000, **72**, 645–651.
34. Dundon, M. L., Brown, G. H. and Capstaff, J. G., A quick test for determining the degree of exhaustion of developers. *J. Soc. Motion Picture Eng.*, 1930, **14**, 389–398.
35. Kitts, E. I., Physics and chemistry of film and processing. *RadioGraphics*, 1996, **16**, 1467–1479.
36. Hall, C. and Schoen, A., Application of the electron microscope to the study of photographic phenomena. *J. Opt. Soc. Am.*, 1941, **31**, 281–285.
37. Liu, S., Wehmschulte, R. J., Lian, G. and Burba, C. M., Room temperature synthesis of silver nanowires from tabular silver bromide crystals in the presence of gelatin. *J. Solid State Chem.*, 2006, **179**, 696–701.
38. Wiley, B., Sun, Y., Mayers, B. and Xia, Y., Shape-controlled synthesis of metal nanostructures: the case of silver. *Chem. – A Eur. J.*, 2005, **11**, 454–463.
39. Van Renterghem, W., Schryvers, D., Van Landuyt, J., Van Roost, C. and De Keyser, R., The influence of silver halide crystal thickness on image tone. *J. Imaging Sci. Technol.*, 2003, **47**, 133–138.
40. Schuette, W. M. and Buhro, W. E., Silver chloride as a heterogeneous nucleant for the growth of silver nanowires. *ACS Nano*, 2013, **7**, 3844–3853.
41. Harris, D. C., Nonlinear least-squares curve fitting with microsoft excel solver. *J. Chem. Edu.*, 1998, **75**, 119.
42. Madaria, A. R., Kumar, A., Ishikawa, F. N. and Zhou, C. W., Uniform, highly conductive, and patterned transparent films of a percolating silver nanowire network on rigid and flexible substrates using a dry transfer technique. *Nano Res.*, 2010, **3**, 564–573.

ACKNOWLEDGEMENTS. We thank DST, MCIT under CEN Phase II, and Space Technology Cell of IISc, Bangalore for financial support.

Received 30 January 2014; revised accepted 1 May 2014

## Field-normalized bibliometric evaluation of leading research institutions in chemistry in China and India

Gangan Prathap\*

CSIR National Institute for Interdisciplinary Science and Technology, Thiruvananthapuram 695 019, India

**Chemistry is the biggest area of research in which India publishes and it is the second biggest for China in recent years. Within this broad research area, the Council of Scientific and Industrial Research (CSIR) is India's biggest single academic research contributor, while the Chinese Academy of Sciences (CAS) is China's biggest player. In this communication, we use field-normalized bibliometric indicators from the latest (2013) release of SCImago Institutions Rankings World Reports to show that while the leading institutions from CSIR are showing a declining trend in the quality of research output, their counterparts from CAS are rapidly improving on both quality and quantity terms.**

**Keywords:** Bibliometric indicators, chemistry, field-normalization, research institutions ranking.

THE Council of Scientific and Industrial Research (CSIR) and the Chinese Academy of Sciences (CAS) are the premier R&D agencies in India and China respectively. While the former has 38 constituent units (laboratories, centres, institutes, etc.), the latter has 124 institutions. In both agencies, institutes dedicated to research in the broad area of chemistry are prominent for their output and quality of research. In India, chemistry is the area in which the largest output is seen, while in China it is the second largest area of research (after engineering). Within the broad research area of chemistry, CSIR and CAS are the biggest single academic research contributors for India and China respectively.

Most bibliometric exercises are based on using publication counts and citation-based statistics which do not account for varying citation practices in different disciplines<sup>1</sup>. Schubert and Braun<sup>1</sup> pointed out that comparative assessment of scientometric indicators is greatly hindered by the different standards valid in different science fields and sub-fields. Indicators from different fields can be compared only after first gauging them against a properly chosen reference standard, and thereafter their relative standing can be estimated. This makes comparison and benchmarking of laboratories difficult unless some form of field-normalization is implemented. The SCImago Institutions Rankings (SIR) World Reports<sup>2</sup> (<http://www.scimagoir.com/>) present secondary bibliometric data in

\*e-mail: gp@niist.res.in